11

Fatigue Life Assessment for Lead-Free Solder Joints

Masaki Shiratori and Qiang Yu

Yokohama National University, Japan

Abstract The authors will indicate the basic reliability problems associated with use of lead-free solder joints. They investigated the thermal fatigue reliability of lead-free solder joints, and focused their attention on the formation of the intermetallic compound and its effect on the initiation and propagation of the fatigue cracks. An isothermal fatigue test method was used to improve the efficiency of fatigue study. Several lead-free solder alloys, Sn-Ag-Cu, Sn-Ag-Cu-Bi, Sn-Cu and Sn-Zn-Bi, were investigated.
It was found that there were two kinds of major failure mode in lead-free solder joints: the solder bulk fatigue mode, and the interface fatigue mode. It was found also that the mode shift of the fatigue crack was affected by not only the properties of the intermetallic layer, but also by the tensile strength of the solder material. In order to investigate the influence of plating treatment on the fatigue strength of Sn-Zn-Bi solder joint, specimens with Ni/Au or Cu plating treatment on Cu-pad were used. Through a series of isothermal mechanical shear fatigue tests and FEM (Finite Element Method) analysis, it has been found that the fatigue life of Sn-Zn-Bi solder joint was greatly affected by the environmental temperature and plating conditions.

11.1. INTRODUCTION

Surface mount technologies, such as BGA (Ball Grid Array), CSP (Chip Size Package), and flip-chip, have been adopted in many electronic devices: computers, household electric appliances, and so forth. The tendency in the developments of surface mount technologies is characterized by miniaturization, performance enhancement, and the higher pin count. In addition, it is crucial that lead is removed from the solder joints. There is a need to establish regulations for the removal of Pb, especially in European countries and Japan. Many studies have been carried out recently to develop technologies for replacing Sn-Pb solder with the lead-free ones.

The authors have studied, and established an evaluation method for thermal fatigue strength for the BGA structure of the Sn-Pb eutectic solder [1–10]. It became clearer that conventional Sn-Pb eutectic solder has many merits, such as a low melting point, good wettability and high electric and mechanical reliability. It is difficult to find a lead-free material that has superior or comparative characteristics compared with the eutectic solder. At

the moment, the most favorable candidates for the lead-free solder materials are Sn-Cu for the flow soldering, and Sn-Ag-Cu, Sn-Ag-Bi and Sn-Zn-Bi for the reflow soldering. Using these solders one can achieve almost as close a reliability level as using Sn-Pb eutectic solder. There is a concern, however that the intermetallic compound formed by the thermal fatigue cycle might seriously affect the thermal fatigue strength under some special conditions [11,12].

The authors have paid attention to the role of the intermetallic compound formation between the solder bulk and the Cu-pad due to thermal cycling, in Sn-Ag-Cu (Bi), Sn-Cu and Sn-Zn-Bi lead-free solder materials [11–15]. We addressed the relation between the intermetallic compound and the thermal fatigue strength, and the relation between the mechanical properties of solder materials and the fatigue failure modes in the solder joints.

11.2. THE INTERMETALLIC COMPOUND FORMED AT THE INTERFACE OF THE SOLDER JOINTS AND THE Cu-PAD

Figure 11.1 shows an enlarged view of the microstructure around the interface of a solder bulk material and the Cu-pad. The intermetallic compound is formed at the interface if the Cu-pad is not plated by Ni. The components of the compound are Cu-Sn (Cu6-Sn5 or Cu3-Sn), in the case of eutectic solder, and Sn-Ag-Cu (Bi). The fatigue fracture mode of the solder joints, in which the intermetallic compound is remarkably formed, depends upon the solder materials, processing conditions, testing conditions, and so forth.

The fracture modes can be roughly classified into the following three types:

(1) Fatigue fracture in the solder bulk layer. It is solder fatigue failure mode. It is caused by the low cycle fatigue due to the repeated nonlinear strain. In this case, the fatigue life assessment can be carried out by using Manson-Coffin's law as a basis [3].
(2) Fatigue failure in the intermetallic compound layer or at the interface of the intermetallic compound and the solder material. It is interface fatigue mode. This failure mode is caused by the decrease in ductility due to the growth of the intermetallic compound layer.
(3) Peeling failure of the Cu-pad from the printed circuit board. This is caused by the stress concentration.

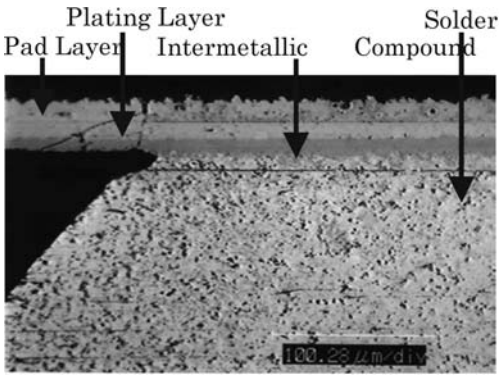

FIGURE 11.1. Structure of solder joint.

For the mode (2), the factors affecting this mode can be due to the following causes:

(1) For the intermetallic compound layer:

- Growth of the intermetallic compound under the reflow process;
- Growth of the intermetallic compound due to the dwell time at high temperature during the thermal fatigue test;
- Repeated stress concentration at the intermetallic compound layer at low temperature during the thermal fatigue test.

(2) For failure at the interface of intermetallic compound and the solder layer:

- The growth of the intermetallic compound and the repeated stress concentration;
- The coherency of the grain boundaries between the intermetallic compound and the solder bulk.

It was found that it scarcely happens that the different fracture modes arise simultaneously. In almost all the cases, only one mode of fracture is dominant. Therefore, it is important to investigate the conditions under which each fracture mode dominantly occurs. It has been found that the failure modes can be controlled and then a good guideline can be acquired to develop a new solder material and soldering process. In this paper the authors have paid attention to the difference in fracture mechanism of the solder joints. We investigated the initiation criteria of each fracture mode and the effect of the mechanical properties of solder material on these failure modes.

11.3. MECHANICAL FATIGUE TESTING EQUIPMENT AND LOAD CONDITION IN THE LEAD FREE SOLDER

The isothermal mechanical fatigue test was proposed to evaluate the fatigue reliability of the Sn-Pb solder joints instead of the thermal cyclic test [7,8,10,11,16]. It has been confirmed that the fatigue life of solder joints under power cycling can be predicted by the same Manson-Coffin's curve given by the isothermal mechanical fatigue tests. The shift in the failure modes can be checked by comparing the experimental results of the fatigue life with the value predicted from the fatigue life curve for the solder failure mode. If the fatigue life of a solder joint is much shorter than the predicted value, that means that the failure mode has changed from the "good," cohesive, failure mode to the interface failure mode or the other bad mode. The consistency of these two kinds of test methods has sufficiently been taken for the Sn-Pb solder joints case, where the failure mode was almost always the solder fatigue mode. However, the growth of the intermetallic compound in high-temperature dwell time must be considered, because the interface failure mode may become one of the major modes, when a lead free solder material is used. In this study, in order to investigate the interface fatigue behavior using the isothermal fatigue test method, a specimen with lead-free solder was heat-treated before the test to accelerate the growth of intermetallic compound. And then the cyclic mechanical deformation was directly given to the specimen to measure its fatigue life.

Figure 11.2 shows the schematic illustrations of isothermal mechanical fatigue test equipment used in this study. The specimen was fixed to the jigs by bonding both upper and lower surfaces. Then cyclic shear displacement was applied repeatedly to the upper jig. A displacement controlled fatigue test was carried out by applying triangular waves with a

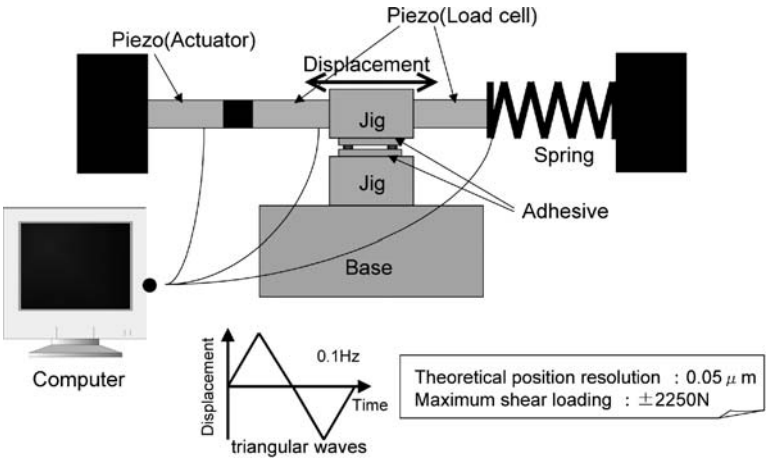

FIGURE 11.2. Isothermal fatigue-testing equipment.

constant displacement rate. The cross-sections of the solder joints were observed through a microscope with high magnifying power (maximum to 3000 magnifications on the display) during the whole fatigue cycles. The relative displacement on the upper and lower surfaces of the solder ball, $\Delta\delta_{re}$, was measured directly and automatically by the digital microscope system. Although there could be some different definitions for the number to failure N_f, in this study, it was defined as the number of cycles when the load measured by a piezo type load cell drops about 10% from the initial level of the reaction load. In order to investigate the stress and strain behavior in the solder joint under the mechanical cyclic loading, the elasto-plastic analyses were carried out by using ANSYS.

11.4. RESULTS OF MECHANICAL FATIGUE TEST

In this study, shear type mechanical fatigue tests were used to examine the failure modes and fatigue strength of lead free solder joints. Figure 11.3 shows the structure of a shearing type solder joint. Because the width of the solder layer is much longer than its height, this kind of solder joint could reduce the stress and strain concentrations at the edge of the solder layer. The lead-free solder materials used in this study are Sn-Cu-Ni, Sn-2.9Ag-0.5Cu-3Bi, and Sn-8Zn-3Bi. The test specimens were heat-treated before the testing by holding at 150°C for 200 hours to accelerate the growth of intermetallic compound as in the thermal cycle test. The Sn-8Zn-3Bi specimen was heat-treated at 110°C for 300 hours. The fatigue life of each solder joint was evaluated from the results of elasto-plastic analyses and the mechanical fatigue test. The results of the measured fatigue life for each lead free solder joint are shown in Figures 11.4–11.9.

Figure 11.4 shows that Sn-Cu-Ni solder joints have almost identical fatigue strength whether they were heat-treated or not. The fatigue failure mode was observed in details by the microscope to verify the above results. It was observed that the crack initiated within the solder bulk (solder fatigue mode) for both cases, as shown in Figure 11.5.

Figure 11.6 shows that the results of the fatigue life of the heat-treated specimen of Sn-2.9Ag-0.5Cu-3Bi decreased a little in comparison with the specimen that was not heat-treated. It was shown that the fatigue cracks were initiated within the matrix of sol-

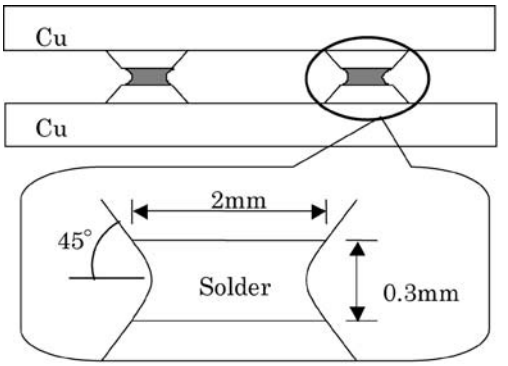

FIGURE 11.3. Structure of shearing type specimen.

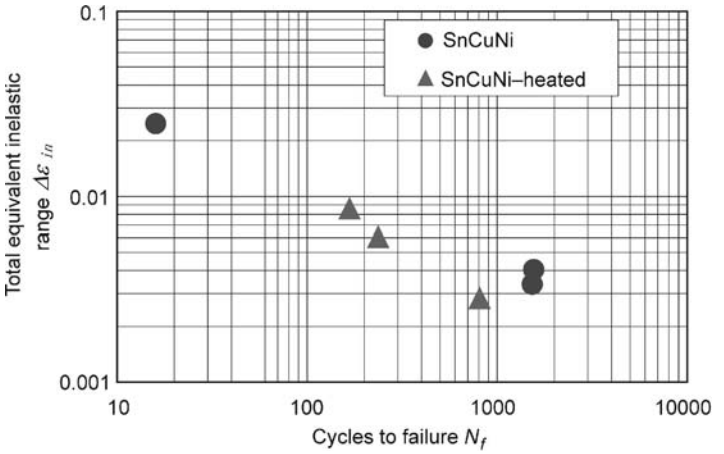

FIGURE 11.4. S–N curves of Sn-Cu-Ni solder joints.

der material (solder fatigue mode) in the case of not heat-treated specimen. On the other hand, for the heat-treated specimen, the fatigue cracks initiated in the solder layer where very close to the interface between the intermetallic compound layer and solder bulk. The cracks propagated with a path parallel to the interface (similar to an interface fatigue mode). This case was called solder/interface fatigue mode. Optical micrographs are shown in Figure 11.7.

Figure 11.8 shows that the fatigue life of the not heat-treated Sn-8Zn-3Bi specimen was much longer than that of the specimen heat-treated at 150°C for 200 hours. It was observed that the cracks initiated in the solder bulk (solder fatigue mode) in the case of not heat-treated specimen, and the cracks in the specimen heat-treated for 300 hours at 110°C initiated and propagated with the similar mode of Sn-2.9-0.5Cu-3Bi solder joint. However, the fatigue cracks initiated at the interface between the intermetallic compound layer and solder (a true interface fatigue mode) for the case of specimen heat-treated for 200 hours at 150°C. It was assumed that in this case there existed a reaction layer (CuSn) newly grown between the solder and intermetallic layer (ZnCu), and the cracks just started in this new layer. Figures 11.9 show the optical micrographs of the fatigue fracture modes of Sn-Zn-Bi solder joints. The above results showed that the shift in the fatigue fracture mode in the

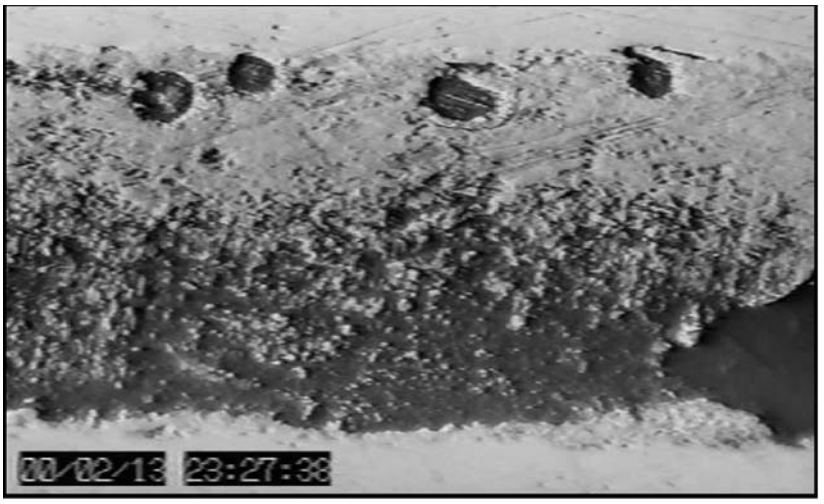

(a)

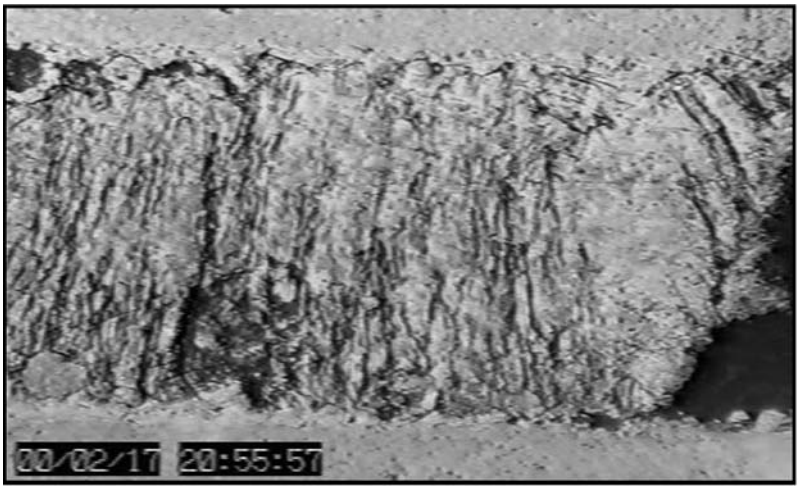

(b)

FIGURE 11.5. Optical micrograph of fatigue crack in Sn-Cu-Ni solder joints. (a) Solder joint without high temperature exposure. (b) Solder joint after 200 hours exposure at 150°C.

solder joints from the cohesive failure in the solder to the interface mode might result in a significant decrease in the fatigue life.

The other type of fatigue test specimen used in this study is the BGA solder joints, where a dummy component was connected to a Cu-plated substrate by two lead-free solder balls. The lead-free solder materials used in these specimens are Sn-3.5Ag-0.75Cu and Sn-3.5Ag-5Bi. These specimens were heat treated by holding at 120°C for 360 hours to grow the intermetallic layer, and the specimens are classified into four types (Table 11.1).

Figure 11.10 shows the results obtained by the mechanical fatigue tests and elasto-plastic analyses. The figure shows the following:

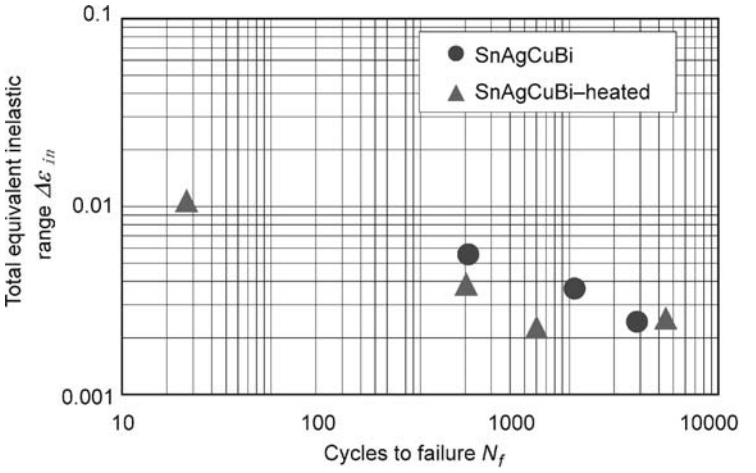

FIGURE 11.6. S–N curves of Sn-2.9Ag-0.5Cu-3Bi solder joints.

TABLE 11.1.
Types of BGA specimens.

	No heat treatment	Heat treated
Sn-3.5Ag-0.75Cu	B1	B2
Sn-3.5Ag-5Bi	C1	C2

(1) the effect of heat treatment may be negligible in the case of Sn-3.5Ag-0.75Cu solder joints;
(2) the fatigue lives of the heat treated specimen of Sn-3.5Ag-5Bi (C2) decreased remarkably.

Optical micrographs of the BGA specimens after the fatigue test are shown in Figures 11.11 and 11.12. Similar to Sn-Cu-Ni solder joints, the fatigue cracks in both kinds of BGA Sn-3.5Ag-0.75Cu joints (B1 and B2) started and propagated within the solder bulk layer. It means that since Sn-Ag-Cu solder joints broke with a solder fatigue mode, the fatigue life was not affected by the conditions of reaction interface between the solder and the Cu pad. The situation was the same for the Sn-3.5Ag-5Bi specimen without heat treatment (C1), where the remarkable growth of the intermetallic compound layer could not be observed. On the other hand, the interface in heat-treated Sn-3.5Ag-5Bi solder joints (C2), where the remarkable growth of intermetallic compound layer was observed, broke and the interface fracture mode resulted in great decease in the fatigue life.

11.5. CRITICAL FATIGUE STRESS LIMIT FOR THE INTERMETALLIC COMPOUND LAYER

As a result of the mechanical fatigue test, it was found that the fatigue failure mode of the solder joints depended upon the solder material and the condition of the reaction layer. To explain this phenomenon, the authors have observed the nonlinear stress–strain characteristics of solder materials (Figure 11.13).

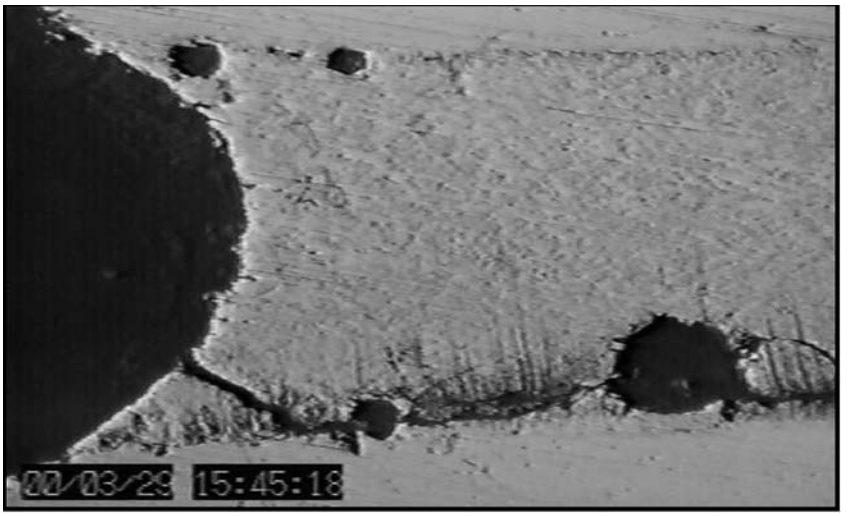

(a)

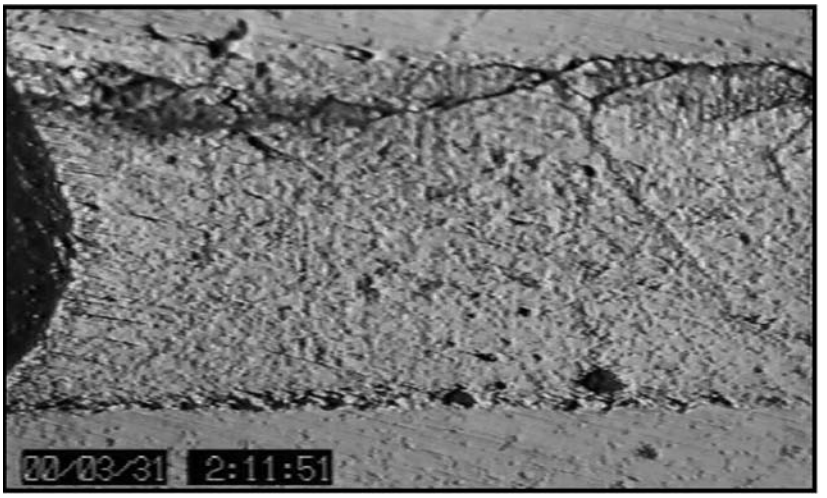

(b)

FIGURE 11.7. Optical micrograph of fatigue crack in Sn-2.9Ag-0.5Cu-3Bi solder joints. (a) Solder joint without high temperature exposure. (b) Solder joint after 200 hours exposure at 150°C.

The figure shows that the flow stress of Sn-3.5Ag-5Bi is remarkably higher than those of Sn-Pb and Sn-3.5Ag-0.75Cu. It means that Sn-3.5Ag-0.75Cu like Sn-37Pb has a much lower yield stress to let the solder layer to deform easily as a cushion for hard and fragile intermetallic compound layer. The stress applied on the interface layer can not increase high enough to break the reaction layer (intermetallic layer) during the fatigue test. However, lead-free materials with rich Bi are much harder than the Sn-Pb eutectic solder and more difficult to deform, and the higher yield stress may cause a very critical stress level on the interface layer. This may be the reason why a very fast fracture, which was closer to a brittle fracture than to a slow ductile fracture, occurred in and along the intermetallic compound. However, this kind of brittle fracture just propagated with a very

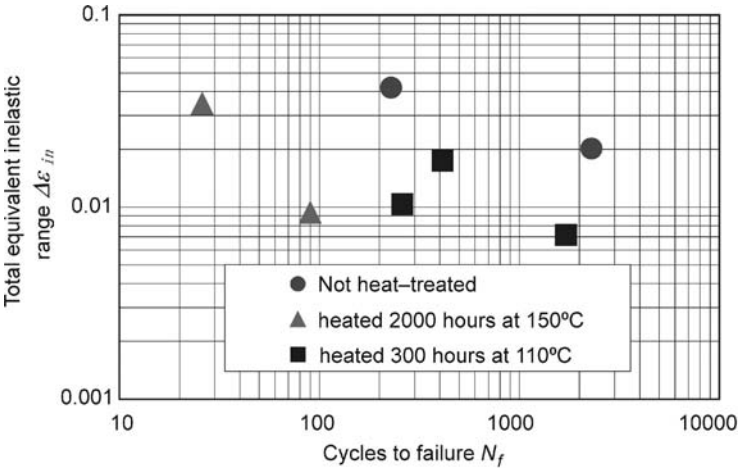

FIGURE 11.8. S–N curves of Sn-8Zn-3Bi solder joints.

TABLE 11.2.
Relation of fracture mode to tensile strength.

Solder material	Tensile strength (MPa)	Fracture mode
Sn-37Pb	38	Solder
Sn-Cu-Ni	35	Solder
Sn-3.5Ag-0.75Cu	49	Solder
Sn-2.9Ag-0.5Cu-3.0Bi	58	Solder/Interface
Sn-8Zn-3Bi	66	Solder/Interface (110°C) Interface (150°C)
Sn-3.5Ag-5Bi	68	Interface

small scale in every cycle because the displacement controlled load could cause of stress relaxation quickly after the crack propagation. In the case of the specimen C2, there existed the well-grown intermetallic compound layer due to the exposure at high temperature. The high stress level due to the high yield stress of Sn-Ag-5Bi caused the brittle fracture at the intermetallic compound (interface fatigue mode). This resulted in the remarkable decrease in the fatigue life. It can be assumed that the same brittle fracture occurred also in Sn-8Zn-3Bi joints after 200 hours exposure at 150°C, since the similar intermetallic compound layer to Sn-3.5Ag-5Bi joint existed at its interface. However, Sn-8Zn-3Bi could break only the interface of the ZnCu intermetallic compound layer in the solder joint after 300 hours exposure at 110°C. Because the toughness of the ZnCu intermetallic compound is said to be higher than that of SnCu, this failure mode may not be a big problem.

The relation between the tensile strength (flow strength at 2% strain) and the fatigue fracture mode of each solder joint is shown in Table 11.2. The fatigue fracture mode shifts as the solder hardens, from the solder mode to the interface mode, it is necessary to pay attention to the stress concentration, as well as to the strain behavior when one wants to assess the thermal fatigue strength of the solder joints with intermetallic compound layers [6]. Figure 11.14 shows the distributions of Mises equivalent stresses at the interface layer in the solder joint of Sn-37Pb, Sn-3.5Ag-0.75Cu, and Sn-3.5Ag-5Bi, respectively.

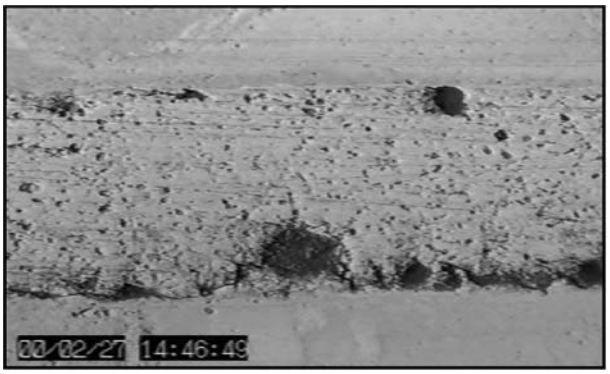

(a)

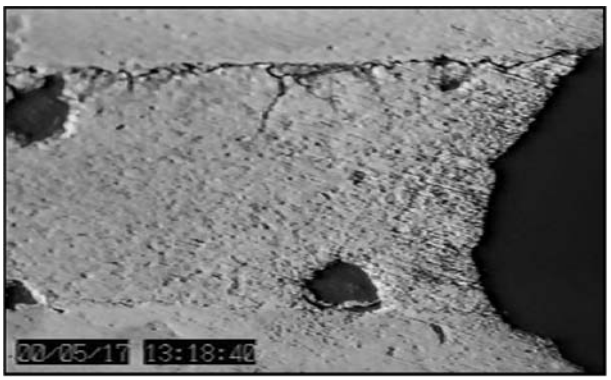

(b)

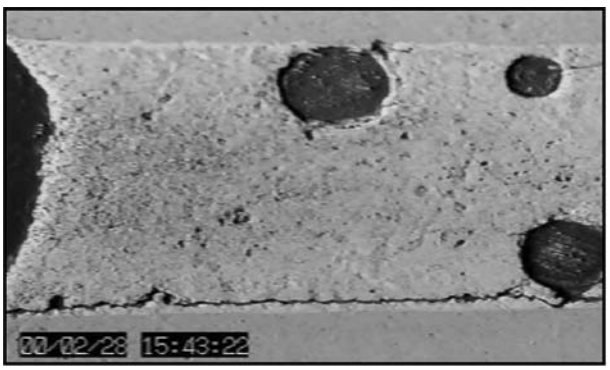

(c)

FIGURE 11.9. Optical micrograph of fatigue crack in Sn-8Zn-3Bi solder joints. (a) Solder joint without high temperature exposure. (b) Solder joint after 300 hours exposure at 110°C. (c) Solder joint after 200 hours exposure at 150°C.

Stress concentration at the end of the interface in the Sn-37Pb solder joint is the lowest, and that of the Sn-3.5Ag-5Bi is the highest. The maximum stresses are limited by the yield stresses of the solder materials. It is impossible for the maximum stresses to increase over the yield stresses. The maximum stress of each kind of solder joint corresponds to the sol-

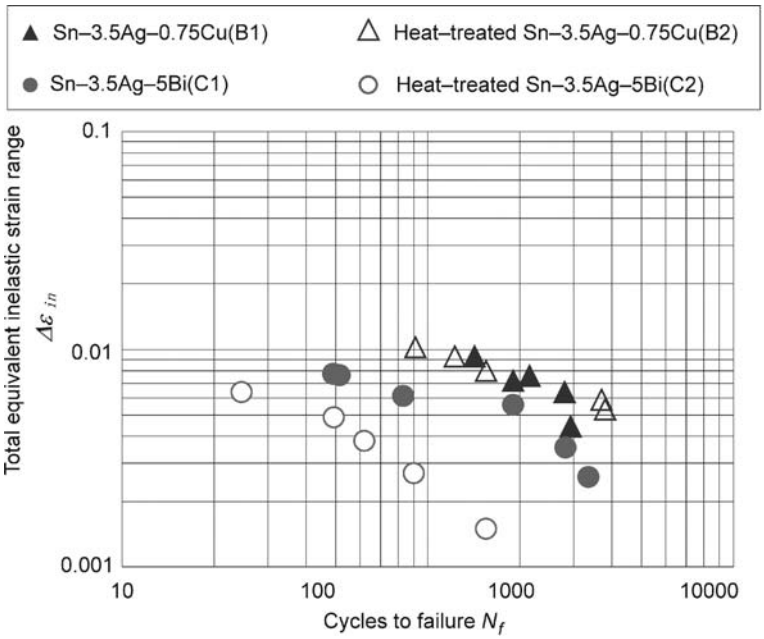

FIGURE 11.10. S–N curve of BGA solder joints.

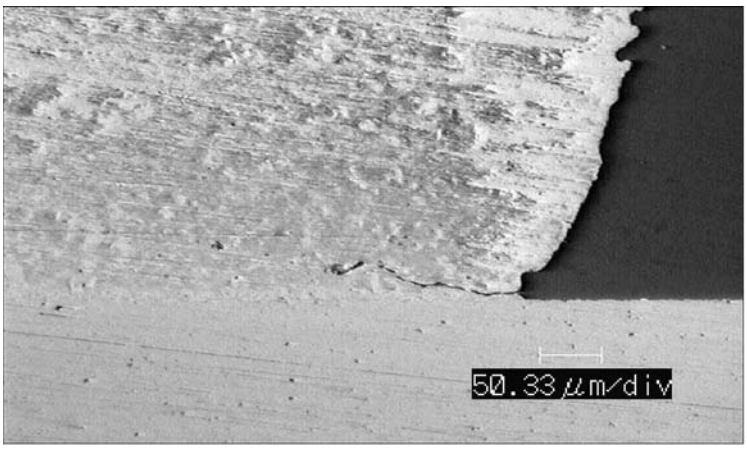

FIGURE 11.11. Crack in Sn-3.5Ag-0.75Cu BGA solder joint (B2).

der strength stress as shown in Table 11.2. This is because almost all the stress components in the solder domain are continuous to those in the intermetallic layer at the interface, and the stresses arising in the solder domain are constrained by its nonlinear stress–strain relationship. Therefore, there is no singularity problem for the stress distribution for the plastic deformation case.

Based upon the above considerations and also from the results of the mechanical fatigue test, it can be assumed that there might exist a critical stress (or tensile strength of solder material) limit against interface fatigue fracture mode for each intermetallic com-

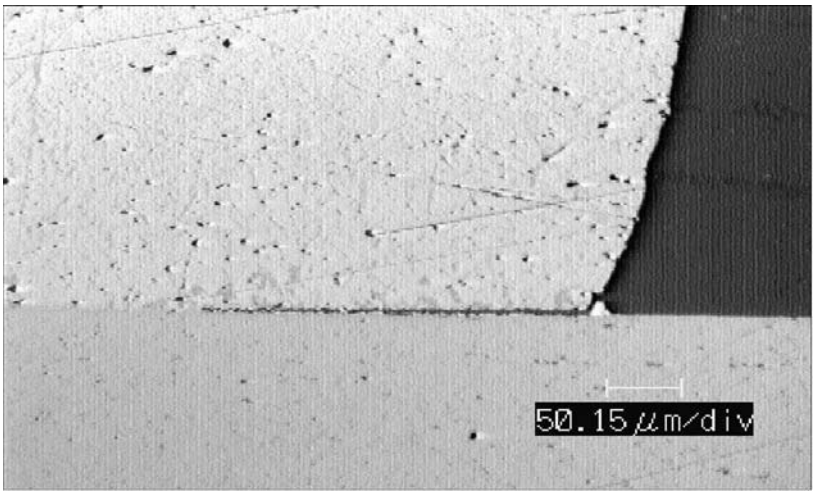

FIGURE 11.12. Crack in Sn-3.5Ag-5Bi BGA solder joint (C2).

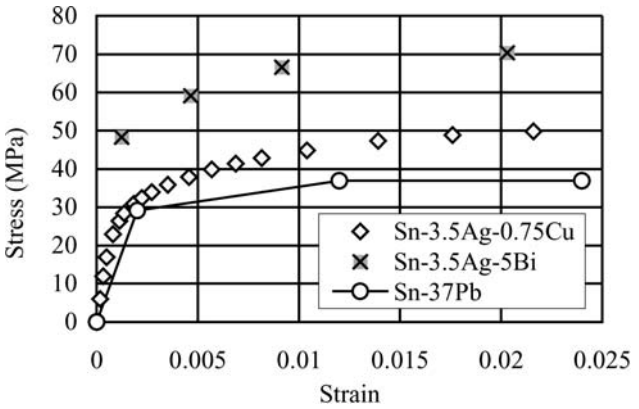

FIGURE 11.13. Stress–strain curve of solder materials.

pound SnCu and ZnCu. If the tensile strength of solder is lower than the limit, the fatigue cracks will appear within the solder bulk layer. This is the solder fatigue failure mode. The fatigue life of these solder joints is dominated by Manson-Coffin's law in the bulk solder material. However, if the tensile strength is higher than this limit, the brittle interface fatigue occurs much earlier than the solder fatigue life. This is the interface fatigue mode.

Summarizing the above results, we conclude that the critical stress limit for intermetallic SnCu should be drawn between the maximum stresses of Sn-3.5Ag-0.75Cu and Sn-3.5Ag-5Bi as shown in Figure 11.15, or, to be exact, the critical stress should be set close to the tensile strength of Sn-2.9Ag-0.5Cu-3Bi, 58 MPa, because it has been checked that the major failure mode of this solder joints was something like a mixed mode of solder and interface modes (solder/interface mode). This means that the failure mode of Sn-2.9Ag-0.5Cu-3Bi joints located just at the borderline of the two major failure modes. In the case of Sn-3.5Ag-0.75Cu, most of the cracks initiated within the solder layer, since its tensile

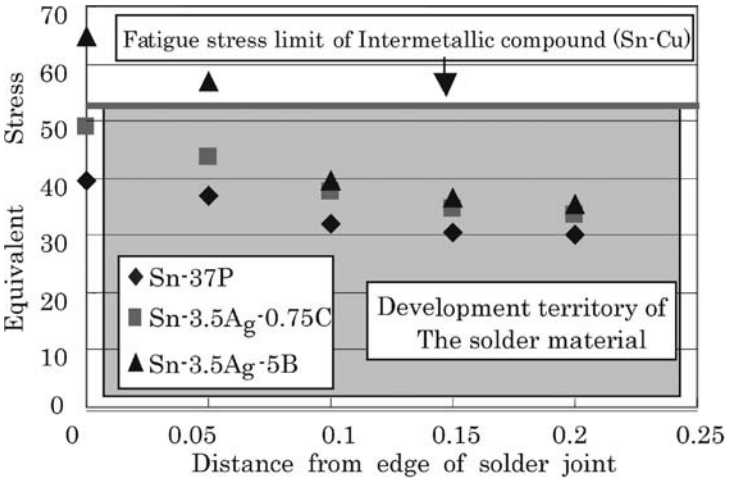

FIGURE 11.14. Distributions of Mises equivalent stresses.

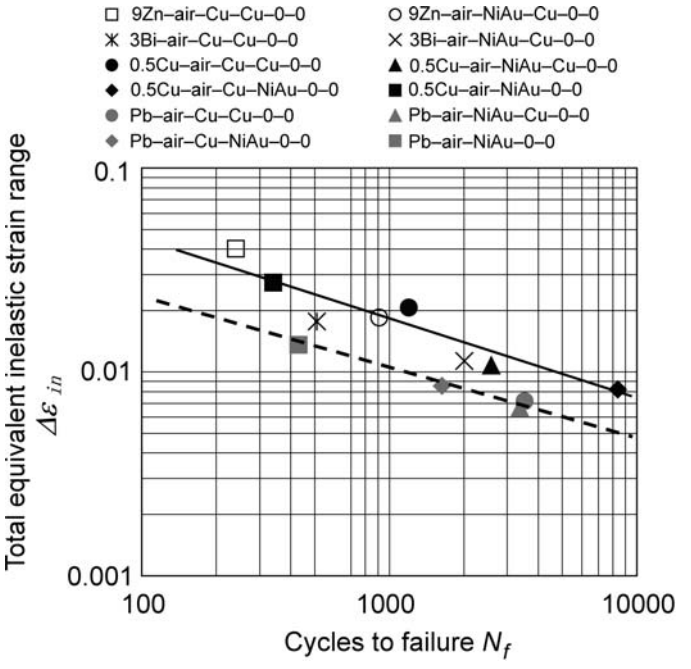

FIGURE 11.15. Fatigue life of Sn-Zn solder joints with initial state.

strength limits the maximum equivalent stress concentration at the end of the solder joint not to cross over the critical stress. For the same reason, it was very rare to find an interface fatigue failure mode in the Sn-Pb solder joints.

On the other hand, in the case of Sn-3.5Ag-5Bi, the tensile strength is higher than the critical stress, and, as a result, the brittle fracture at the intermetallic compound caused a

great decrease in the fatigue life. Based upon the results shown in Figures 11.8 and 11.9, it can be assumed that the limit stress for ZnCu is roughly between 60 to 68 MPa.

The above consideration shows that the reliability engineers have to think of the balance of the strengths of both the intermetallic compound and the solder matrix, if they want to achieve high enough fatigue reliability of a lead-free solder joint. In order to avoid the brittle fracture at the intermetallic compound layer, one has to consider the flow characteristics of the lead-free material, or to manage to prevent the growth of the intermetallic compound.

11.6. INFLUENCE OF THE PLATING MATERIAL ON THE FATIGUE LIFE OF Sn-Zn (Sn-9Zn AND Sn-8Zn-3Bi) SOLDER JOINTS

In order to investigate the influence of plating treatment on the fatigue strength of Sn-Zn solder joints, the specimens with Ni/Au or Cu plating treatment on the Cu-pad at the side of substrate were prepared. These specimens were aged for 200, 500, 1000 hours at 85, 125, 150°C to investigate the influence of the fatigue strength due to the growth of the intermetallics. Some specimens were exposed to the high-humidity/temperature environment (85%/85°C).

Figure 11.15 shows the results of the solder joints without high temperature aging. As shown in Figure 11.15, the specimen has been characterized and named by solder material [9Zn, 3Bi, 0.5Cu, Pb], reflow environment [air, N_2], plating materials on the substrate side [Ni/Au, Cu], plating materials on the chip side [Ni/Au, Cu], aging temperature [85°C, 125°C, 150°C, 85°C (85%)], aging time [100 h, 200 h, 500 h, 1000 h]. Figure 11.15 shows the relation between the fatigue life N_f and inelastic equivalent strain range $\Delta\varepsilon_{in}$ of initial state (non-aging) for Sn-9Zn, Sn-8Zn-3Bi, Sn-3Ag-0.5Cu and Sn-Pb CSP solder joints. In Figure 11.15, the dotted line represents the fatigue life due to the mechanical shear fatigue test for Sn-Pb solder as a reference. The solid line expresses the result of Sn-3Ag-0.5Cu solder. It was found that Sn-9Zn and Sn-8Zn-3Bi solder, without aging, have similar fatigue strength to Sn-3Ag-0.5Cu solder.

Figure 11.16 shows the fatigue strength of a Sn-9Zn specimen. The results of the fatigue test are divided into two groups. The dotted line shows the average results of the mechanical shear fatigue test for Sn-Pb solder. The solid line shows the average results of specimen groups with good fatigue mode. Not-aged specimens are located on this line. In the case of the Cu plating specimen, the aged specimens have similar fatigue strength to the initial state (non-aging) specimens, even if heat treatment was carried out at 150°C for 1000 hours. If the specimens with Ni/Au plating treatment were aged at 85°C for 1000 hours or a much higher temperature condition, these fatigue strength decreased. Although fatigue strength becomes lower, they have the almost identical fatigue strength with Sn-Pb solder (dotted line). However, when the specimens were exposed in the high-humidity/temperature environment, the fatigue strength greatly decreased. This is because Zn is more oxidizable than Sn, Ag, and Cu under high-humidity condition, and the oxidized materials might have a critical effect on the fatigue strength.

Figure 11.17 shows the results of the mechanical fatigue test for Sn-8Zn-3Bi solder joints. The dotted line shows the average results of mechanical shear fatigue test for Sn-Pb solder. The solid line expresses the approximate line of fatigue strength for Sn-8Zn-3Bi solder. The aged Sn-8Zn-3Bi solder specimens with Cu plating treatment show the similar fatigue strength to the initial state (non-aging) specimen. When the specimens with Ni/Au

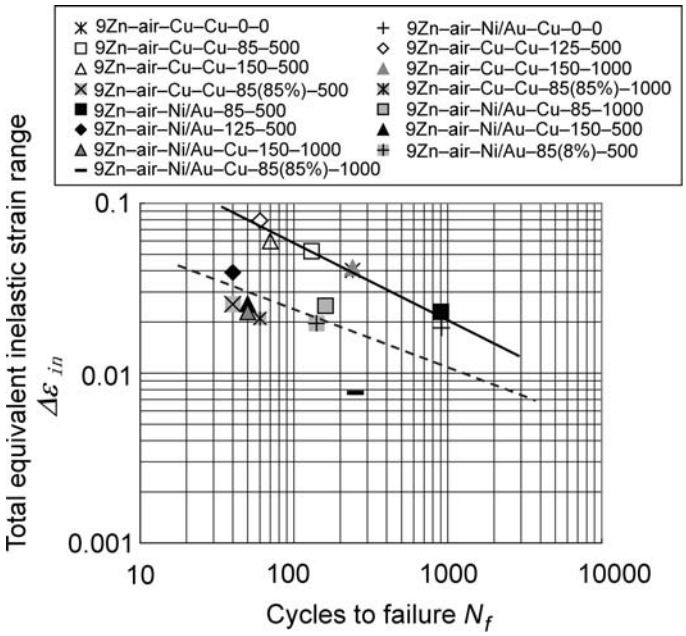

FIGURE 11.16. Fatigue life of Sn-9Zn solder joint.

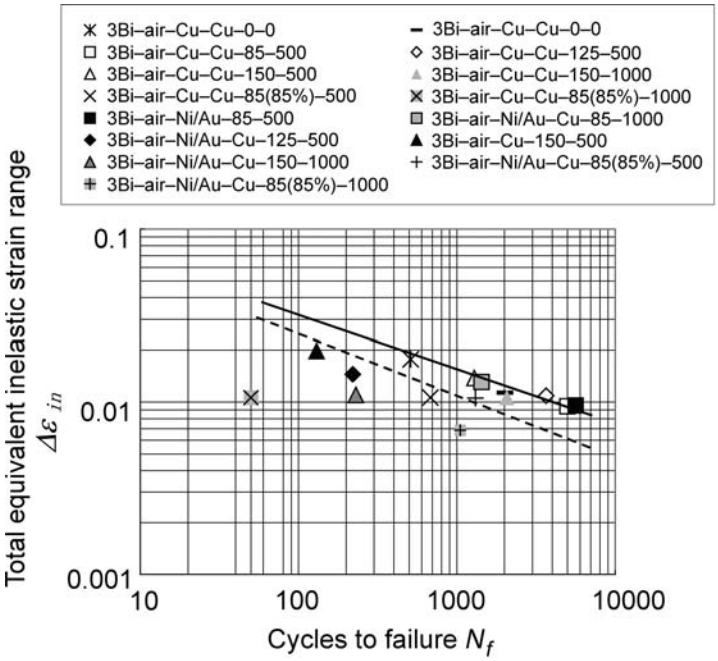

FIGURE 11.17. Fatigue life of Sn-8Zn-3Bi solder joint.

plating treatment were heat aged at 150°C for 1000 hours, their fatigue strength decreased more than that of the Sn-Pb solder. This means the Ni/Au can shelter the growth of the intermetallic layer in Sn-Zn(Bi) solder joints in almost all the cases. One should be very careful when using Sn-Zn(Bi) solder materials for electronics systems that have a high possibility to be used in high humidity environments.

11.7. CONCLUSION

The effect of material property of lead-free solder on the reliability of solder joints was addressed. There exist two kinds of major fatigue failure modes: the solder fatigue mode, and the interface fatigue mode. The interface fatigue mode results in a significant decrease in the fatigue life of solder joints. The mode transition from the solder to the interface is not only affected by the conditions of the reaction layer but is also controlled by the tensile strength of the solder material. The fatigue strength of 95.75Sn-3.5Ag-0.75Cu, Sn-Cu-Ni, Sn-2.9Ag-0.5Cu-3Bi lead free solder joints are not greatly affected by the intermetallic compounds formed during thermal cycles, as the Sn-Pb solder does. Their tensile strengths are lower than the critical limit, and the fatigue fracture is dominated by the solder fatigue mode. However, in the case, when the solder material contains much Bi (over 5%), the crack initiates easily along the interface between the intermetallic compound layer and the solder material. This is because the high-level tensile strength of Sn-3.5Ag-5Bi lead free solder causes severe stress distribution in the interface.

Based upon the obtained results, the possibility of giving guidelines for the new solder material development was suggested by showing the limit stress of fatigue strength of Sn-Cu intermetallic compound. It seems to be possible to obtain a limit stress for the intermetallic compound of Zn-Cu, as well as of Sn-Cu.

In the Sn-9Zn and Sn-8Zn-3Bi solder joints, when their Cu-pads were plated with Cu component, the fatigue strength does not get lower. Though the fatigue strength is reduced when the specimens are plated with Ni/Au and aged at 125°C or less, they have superior fatigue strength that the Sn-Pb solder.

When the Ni/Au plating specimens were aged over 150°C, the fatigue strength at the solder joints decreased greatly. This is caused by the growth of the interface fatigue crack. When the Sn-9Zn and Sn-8Zn-3Bi solder were exposed to high-humidity/temperature environments, their fatigue strength is decreased greatly. From the results, if these lead-free solder materials are used carefully with correct use environment and reflow conditions, practical applications of the Sn-Zn-(Bi) lead-free solder seem to be possible.

REFERENCES

1. Q. Yu and M. Shiratori, A study of mechanical and thermal stress behavior due to global and local thermal mismatch of dissimilar materials in electronic packaging, Proc. of the International Intersociety Electronic Packaging Conference (InterPack'95), EEP-Vol. 10, No. 1, 1995, pp. 389–394.
2. M. Shiratori, Q. Yu, and S.B. Wang, A computational and experimental hybrid approach to creep-fatigue behavior of surface-mounted solder joints, Proc. of the International Intersociety Electronic Packaging Conference (InterPack'95), EEP-Vol. 10, No. 1, 1995, pp. 451–457.
3. M. Shiratori and Q. Yu, Fatigue-strength prediction of microelectronics solder joints under thermal cyclic loading, Proc. of Intersociety Conference on Thermal Phenomena in Electronic Systems (I-Therm V), 1996, pp. 151–157.

4. M. Shiratori and Q. Yu, Life assessment of solder joint, advances in electronic packaging, Proc. of the Advances in Electronic Packaging 1997: Proceedings of the Pacific Rim/ASME International Intersociety Electronic & Photonic Packaging Conference (InterPack'97), EEP-Vol. 19, No. 2, 1997, pp. 1471–1477.
5. Q. Yu, M. Shiratori, and N. Kojima, Fatigue crack propagating evaluation of microelectronics solder joints, Proc. of the Advances in Electronic Packaging 1997: Proceedings of the Pacific Rim/ASME International Intersociety Electronic & Photonic Packaging Conference (InterPack'97), EEP-Vol. 19, No. 2, 1997, pp. 1445–1450.
6. Q. Yu and M. Shiratori, Fatigue-strength prediction of micro-electronics solder joints under thermal cyclic loading, IEEE Transactions on Components, Packaging, and Manufactuting Technology, Part. A, 20(3), pp. 266–273 (1997).
7. Q. Yu, M. Shiratori, and Y. Ohshima, A study of the effects of BGA solder geometry on fatigue life and reliability assessment, Proc. of the 6th InterSociety Conference on Thermal and Thermomechanical Phenomena in Electronic System (Itherm'98), 1998, pp. 229–235.
8. Q. Yu and M. Shiratori, Thermal fatigue reliability assessment for solder joints of BGA assembly, Proc. of the Advances in Electronic Packaging 1999: Proceedings of the Pacific Rim/ASME International Intersociety Electronic & Photonic Packaging Conference (Interpack'99), 1999, pp. 239–246.
9. Y. Kaga, Q. Yu, and M. Shiratori, Thermal fatigue assessment for solder joints of underfill assembly, Proc. of the Advances in Electronic Packaging 1999: Proceedings of the Pacific Rim/ASME International Intersociety Electronic & Photonic Packaging Conference (Interpack'99), pp. 271–275 (1999).
10. M. Ito, Q. Yu, and M. Shiratori, Reliability estimation for BGA solder joints in organic PKG, Proc. of the Advances in Electronic Packaging 2001: Proceedings of the Pacific Rim/ASME International Intersociety Electronic & Photonic Packaging Conference (InterPACK'01), 2001, pp. 1–6.
11. H. Amano and Q. Yu, Effect of interfacial factors on fatigue lifetime of lead-free die-attach solder joint, Proc. of the Advances in Electronic Packaging 2001: Proceedings of the Pacific Rim/ASME International Intersociety Electronic & Photonic Packaging Conference (InterPACK'01), 2001, pp. 1–8.
12. Q. Yu, D.S. Kim, and M. Shiratori, The effect of intermetallic compound on thermal fatigue reliability of lead-free solder joints, Proc. of the Advances in Electronic Packaging 2001: Proceedings of the Pacific Rim/ASME International Intersociety Electronic & Photonic Packaging Conference (InterPACK'01), 2001, pp. 1–8.
13. Q. Yu, D.S. Kim, J.C. Jin, Y. Takahashi, and M. Shiratori, Fatigue strength evaluation for Sn-Zn-Bi lead—free solder joints, Proc. of the ASME International Mechanical Engineering Congress & Exposition (IMECE2002), Paper No. 39686, 2002.
14. D.S. Kim, Q. Yu, T. Shibutani, and M. Shiratori, Nonlinear behavior study on effect of hardening rule of lead free solder joint, Proc. of the Advances in Electronic Packaging 2003: Proceedings of the Pacific Rim/ASME International Intersociety Electronic & Photonic Packaging Conference (Interpack'03), No. 35250, 2003, pp. 1–7.
15. D.S. Kim, Q. Yu, T. Shibutani, N. Sadakata, and T. Inoue, Effect of void formation on thermal fatigue reliability of lead-free solder joints, Proc. of the Ninth Intersociety Conference on Thermal and Thermomechanical Phenomena in Electronic Systems (Itherm 2004), 2004, pp. 325–329.
16. M. Kitano, W. Kumazawa, and S. Kawai, A new evaluation method for thermal fatigue strength of solder joint, ASME, Advances in Electronic Packaging EEP-Vol. 1-1, p. 301 (1992).